

Implementation of homogenization scheme for hardening, localization and fracture of a steel with tailored material properties

Stefan Golling¹, Rickard Östlund¹, Mats Oldenburg¹

Abstract

In recent years the demand of press hardened ultra-high strength steel for safety structures in automobiles has increased and it is estimated that this trend continues. Using a thermo mechanical process with heated and cooled areas in a tool, components with tailored properties can be manufactured. By controlling the cooling rate of the blank different microstructures with varying mechanical properties are achieved. A combination of different material grades based on the microstructure within a component gives additional possibilities in the design of the structural response in a crash situation. The automotive industry and its suppliers require material models to improve the quality and reliability of numerical simulations in the development of press hardened components. A thermomechanical model to predict the phase composition is combined with a homogenization scheme to calculate the hardening, softening and fracture of a press hardened component. Localization occurring in the softening part of the stress strain curve is taken into account by parameters adapted to the element size by introducing an analysis length scale parameter into the material model. The material model is implemented as a user defined material in the commercial finite element code LS-Dyna and validated by comparison to experimental result on component level.

1 Introduction

Trough advances of process modeling within the press hardening technology it is possible to predict the final phase composition of a workpiece after forming and differential cooling. Details of the modeling strategy can be found in [1] and a ready to use material model is implemented in the commercial available finite element code LS-Dyna [2]. Components with predicted microstructure can be used for a crashworthiness analysis in a further simulation step. Impact beams and other passive safety structures can be subjected to loads until fracture. To simulate loading beyond instability of the material a failure and localization model is needed. During initial plastic deformation of a sheet metal, plastic strain is generally distributed uniformly within the volume. If further loaded the plastic strain often localizes, first forming a diffuse neck and finally a localized neck preceding rupture. Once a neck has formed, subsequent straining is confined within the neck. This causes instability and the ductility limit of the material is rapidly reached. Plastic strain rate increase may also be accelerated due to material deterioration caused by ductile plastic damage. Localized necking is a dominant mechanism leading to fracture of safety components in a crash

situation [3]. Instability is also associated with the analysis of localization problems, where under quasi-static loading conditions the equations of incremental equilibrium for rate-independent material descriptions lose ellipticity [4]. As a consequence finite element numerical solutions of localization problems are mesh dependent [5]. The discretization decides the width of the localized band and therefore affects calculated stiffness and strain level within the localized zone. Another issue is the ability of the mesh to accurately resolve localized necking. These matters must be addressed in order to successfully use a strain based failure criterion for problems where localized necking is a probable mode of deformation. A methodology suggested in [6] is adopted here where constitutive and failure parameters are adapted to element size by introducing an "analysis" length scale into these equations. Analysis length is not viewed as a material parameter but rather as a coupling between local plastic strain and the plastic strain calculated with a certain mesh size. [3] In previous studies the strain acting in every phase is not decomposed [1] or only the macroscopic stress-strain behavior is taken into account [3][6]. Using a micromechanical homogenization scheme it is possible to decompose the macroscopic strain into local strain acting in every phase. The homogenization approach used is described by Mori and Tanaka [7] and uses the Eshelby inclusion theory [8]. Eshelby's theory assumes an ellipsoidal inclusion in an infinite matrix. Computing the macroscopic material properties by such an average-field theory is comparable to solving a representative volume element at every integration point. With distinct strains in every phase a more accurate modeling of localization and fracture depending on the phase composition is possible. The mesh dependency as another issue of localization and fracture problems is resolved using an analysis length scale factor. The implementation of the Mori-Tanaka homogenization scheme and its interpretation by Lielens are described in [9] and [10].

2 Homogenization schemes based on Eshelby's solution for inclusions and inhomogeneities

Many mean field methods used in the micromechanical modelling of materials are based on the work of Eshelby [8]. Eshelby studied the stress and strain distributions in homogeneous media and assumed that inhomogeneities in the composite are far apart from each other and no interactions between them occur. With these assumptions every inhomogeneity can be treated as if it exists in a homogeneous matrix. If an elastic body with elastic moduli \mathbf{D}_0 contains an ellipsoidal inhomogeneity with elastic moduli \mathbf{D}_1 , let the body be subjected to a surface traction on the boundary of it. The stress field in the boundary can be evaluated. For the case that the elastic moduli of matrix and inhomogeneity are equal the stress field would be uniform throughout the body. Using the principle of linear superposition the stress field in the body can be obtained if the elastic moduli differ from each other. An inhomogeneity is perturbing the stress and strain field in a body, to solve for the stresses and strains the so-called equivalent inclusion method is applied introducing an eigenstrain into the calculation. The eigenstrain ϵ^* is related to the perturbed strain field ϵ by the Eshelby tensor \mathbf{S} .

$$\epsilon = \mathbf{S}\epsilon^* \quad (1)$$

Eshelby's inclusion tensor is computed using the aspect ratio of the axes of an ellipsoid. In the present paper Eshelby's tensor is calculated for three different cases. In the first case the inclusion has a spherical shape. The second case assumes a penny shaped inclusion, the in plane half axes are equal and the half axis in thickness direction is assumed to be infinit small. In a third case Eshelby's tensor is calculated for a flat ellipsoidal shape, in plane half axes are equal and through thickness half axis is taken as a fraction of the in plane axes. The first two cases are solved to obtain analytical expressions for Eshelby's tensor. For the third case the general expression for Eshelby's tensor for ellipsoidal inclusion is solved. For detailed information about Eshelby's inclusion theory see [11] or [12]. The material response is therefore isotropic. A property of the Eshelby tensor is its independence from the size of the inclusion, the only variables used to calculate the tensor are the elastic properties of the phases. In [9] it is proposed good numerical predictions are obtained if Eshelby's tensor is computed using isotropic moduli. The general expression of the elastic moduli \mathbf{D} is

$$\mathbf{D} = 3\kappa_t \mathbf{I}^{vol} + 2\mu_t \mathbf{I}^{dev} \quad (2)$$

where variables κ_t and μ_t are the tangent bulk and shear moduli. The Tensors \mathbf{I}^{vol} and \mathbf{I}^{dev} are the volumetric and deviatoric operator, notation according to [9]. For spheroidal inclusions and isotropic moduli the Eshelby tensor is defined only by the tangent Poisson's ratio ν_t

$$\nu_t = \frac{3\kappa_t - 2\mu_t}{2(3\kappa_t + \mu_t)} \quad (3)$$

where the tangent bulk and shear modulus can be calculated according to

$$\kappa_t = \kappa, \mu_t = \mu \left[1 - \frac{3\mu}{h} \right] \quad (4)$$

where h is the hardening modulus [9].

The effective properties of a multi-phase composite are obtained by the properties of the constituents, the volume fraction of them and the strain concentration tensors relating constituent to composite. A standard averaging scheme is used to relate phase properties to composite properties according to

$$\langle f \rangle = \sum_{i=0}^N c_i \langle f \rangle_i \quad (5)$$

where c_i is the volume fraction of the phase and f a placeholder for a property, e.g. stress. For a typical inhomogeneity in the composite, the effects of other inhomogeneities are communicated to it through the strain and stress fields in its surrounding matrix material. Although the strain and stress fields are different from one location to another in the matrix the averages $\bar{\epsilon}_0$ and $\bar{\sigma}_0$ represent good approximations of the actual fields in the matrix surrounding each inhomogeneity [12]. The strain in the i -th inhomogeneity is related to the average strain in the matrix phase by

$$\epsilon_i = \mathbf{B}_i \bar{\epsilon}_0 \quad (6)$$

where \mathbf{B}_i represents the local strain concentration tensor. The Mori-Tanaka strain concentration tensor for multi-phase materials is used throughout all simulations.

$$\mathbf{B}_i = \left[\mathbf{I} + \mathbf{S} : (\mathbf{D}_0^{-1} : \mathbf{D}_i - \mathbf{I}) \right]^{-1} \quad (7)$$

2.1 Double inclusion model

The double inclusion model was first proposed by [13] and was extended by [14]. In the model, an inclusion is wrapped into another inclusion of different stiffness. These two inclusions share the same center, symmetry axis and aspect ratio, the volume ratio is equal to that of inclusion and matrix in the composite. The inclusions are embedded into an outer material with a stiffness to be chosen by the user. The choice of using the effective stiffness for the outer material yields the self-consistent model. In the same way the outer material can be chosen to have the stiffness of the actual matrix material or of the real inclusion material. In case of the real matrix material as the outer material the Mori-Tanaka model with strain concentration tensor \mathbf{B}_i^l is obtained. If the real inclusion material is used the so called inverse Mori-Tanaka model with strain concentration tensor \mathbf{B}_i^u is found. These two possibilities correspond to upper and lower bounds for the Mori-Tanaka type homogenization. In [14] a homogenization scheme is proposed using an interpolation between the Mori-Tanaka and the inverse Mori-Tanaka scheme. The strain concentration tensor for the composite is then calculated by

$$\mathbf{B}_i = \left[(1 - \xi_{(c_1)}) (\mathbf{B}_i^l)^{-1} + \xi_{(c_1)} (\mathbf{B}_i^u)^{-1} \right]^{-1} \quad (8)$$

In [14] a quadratic interpolation function is proposed

$$\xi_{(c_1)} = \frac{1}{2} c_1 (1 + c_1) \quad (9)$$

3 Implementation in LS-Dyna

The commercially available finite element code LS-DYNA provides the possibility to implement user defined subroutines. The most widely used subroutine is the interface for the implementation of constitutive models. LS-Dyna solves the fundamental conservation equations in continuum mechanics using an explicit time algorithm. In the time integration loop the user routines are called after having calculated strains and strain rates. The user routine calculates the stress field using these input arguments [15]. In previous sections a homogenization scheme and model for the prevention of mesh dependency during localization and fracture is presented. A detailed description of the localization and fracture model is available in [3]. The localization and fracture model is an extension of a commonly used radial return mapping algorithm for isotropic von Mises plasticity as described in e.g. [16]. The homogenization of phases is performed using the elasticity tensor

with tangent shear and bulk modulus and the Eshelby tensor calculated in the radial return subroutine. Strain concentration tensors and stiffness tensors are computed and used to obtain a macroscopic stiffness tensor to update the composite stress. Fracture occurs when the localization function reaches its critical value or the shear failure criterion is fulfilled

$$\int_0^{t_f} \frac{\dot{L}}{L^f} dt = 1, \int_0^{t_f} \frac{\dot{\epsilon}_p}{\epsilon_f} dt = 1 \quad (10)$$

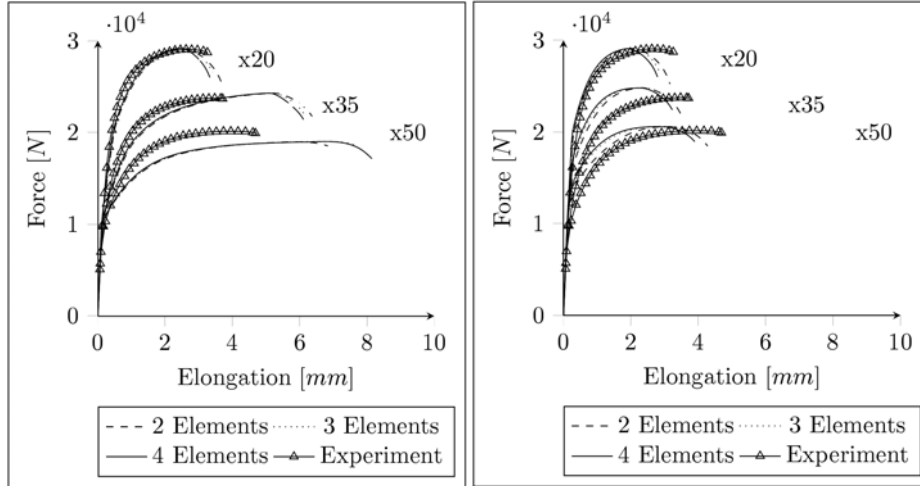
The material model described is intended to be used with shell elements. To account for thickness changes plane stress iteration is included into the algorithm. The hardening part of the flow curve is described by an exponential function. The localization and fracture model uses as well parameters fitted to initial conditions of heat treated blanks. How to obtain those parameters is described in [17], parameters for the model can be found in [3]. Beside parameters describing the flow curve of the material the phase composition of the steel is of importance to predict the mechanical response. Three different phase compositions were produced using varying cooling times in air before quenching the samples in a tool. Microstructure characterization using LOM (Light Optical Microscope) observations lead to the phase composition depicted in table 1.

Table 1: Phase composition of test samples

Sample	Ferrite [volume fraction in %]	Martensite [volume fraction in %]
x20	30	70
x35	50	50
x50	70	30

4 Results

To validate the material model finite element simulation of a tensile test specimen with different phase compositions and mesh sizes and inclusion shapes is performed. The result of the simulation is compared to experimental results performed on a straight uniaxial specimen. The finite element model is discretized with Belytschko-Tsay shell elements (LS-Dyna, type 2) using three different element sizes and square shape in the localization zone. The boundary conditions on one side of the specimen are set to zero and on the other side to linear displacement in accordance with to experimental conditions. The material grades used as input data are HT400 and HT1150. The material HT400, steel 22MnB5 (Usibor by Arcelor Mital), is austenitized at 900°C for about 15 minutes and air cooled prior to testing. Characterization shows a ferritic-perlitic microstructure. Samples HT1150 are made of the same steel and the same austenitization procedure but quenched in a tool, the microstructure of this samples is characterized to consist of martensite. Test specimens with three different phase compositions, see table 1, were produced. All samples were austenitized in the same way as material HT400 and HT1150 but after removing from the furnace air cooled, horizontal lying on pins in the quenching tool, with different holding time before quenching. Test specimens for all material grades are cut perpendicular to rolling direction of the blank.



(a) Spherical inclusion

(b) Penny shape inclusion

Figure 1: Result from FEM analysis for different phase compositions, mesh sizes and inclusion shapes.

Tensile testing results of samples with phase compositions from table 1 show similar elongation and only minor tendency to localization. In figure 1 numerical results for different phase composition, mesh sizes and inclusion shapes are summarized. The model for localization and fracture to minimize the effect of mesh dependency provides good comparability for different mesh sizes, see [3]. Combining the model with the homogenization leads to a certain dependency on phase composition and inclusion shape as can be seen for sample x50 in figure 1a. Hardening of the material using spherical inclusion geometry is underestimated especially for sample x50. This result is expected as Mori-Tanaka type estimates are reported to underestimate the hardening of metals for low volume fractions of inclusion phases. From LOM observations ferrite is seen as continuous phase even for high volume fractions of martensite, this assumption is supported by [18]. Ferrite is therefore assumed as matrix phase for all simulated compositions. For higher volume fractions of martensite the computed hardening is in better agreement with experimental results. Numerical results over predict the elongation for samples x50 and x35 hence fracture values do not correspond to experimental values. For sample x20 the elongation is in good agreement with experimental results but the localization is incorrect. The distinct localization for high volumes of martensite is expected because of the calibrated parameter values for pure martensite which showed pronounced localization. The second case investigated is a change of the inclusion geometry. Eshelby's tensor is calculated for a penny shape, figure 1b compares the obtained result. In general the hardening of the material is higher compared to spherical inclusion results while the elongation before fracture is lower. Introducing an inclusion geometry different from spherical into the material model results in anisotropy. The anisotropy introduced acts in through thickness direction and therefore thinning calculated in plane stress condition is affected but in negligible size.

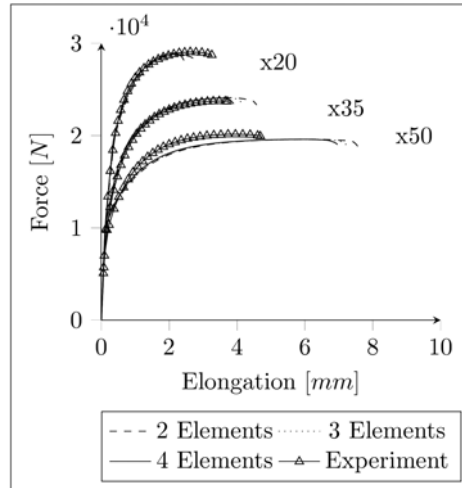


Figure 2: Result from FEM analysis for different phase composition, mesh sizes and ellipsoid inclusion shape.

Spherical and penny shape for geometries describing the inclusion shape are special cases. Choosing a ratio of the in plane half axes to the through thickness half axis of the inclusion between these two cases leads to an ellipsoidal inclusion. Numerical results for an ellipsoidal inclusion geometry are between the results for spherical and penny shape. An example for an ellipsoidal result is shown in figure 2, the aspect ratio of the through thickness half axis is changed to ten percent of the in plane half axes.

3 Conclusion

Three different material compositions were produced using air cooling and tool quenching. A homogenization method to calculate distinct strain in each phase is combined with a phenomenological localization and fracture model to predict the composite response under tensile loading. Numerical results show that the hardening behavior of the steel grades can be well predicted at higher volume fractions of HT1150. The localization and fracture model is possible to combine with the homogenization. Variation of the half axis ratio defining Eshelby's tensor is a way to achieve reasonable agreement between experimentally obtained elongation before fracture and numerical results. A possible explanation for differences between experiment and simulation is the parameters used. Initially all parameters were determined on measurements of sheets with a thickness of 1.2mm but all tensile specimens were cut from sheets with thickness 1.8mm. Numerical results for the composition labeled x50 show a scattered result for the fracture strain. A possible explanation is the analysis length scale factor. The localization band is most likely within the element size for two elements but for smaller elements the band is larger than one element in width.

References

- [1] Åkerström, P.: Modelling and simulation of Hot Stamping. PhD thesis, Luleå University of Technology (2006)
- [2] LS-DYNAR Keyword User's Manual Volume 2 Material Models, (August 29, 2012), pp. 955-969.
- [3] Östlund, R.: Modelling and Characterization of Fracture Properties of Advanced High Strength Steels. Licentiate thesis, Luleå University of Technology, Luleå (2011)
- [4] Needleman, A.: Material rate dependence and mesh sensitivity in localization problems. In: *Computer Methods in Applied Mechanics and Engineering* 67 (1988) No. 1, pp. 69-85.
- [5] Tvergaard, V.; Needleman, A.: Flow localization in the plane strain tensile test. In: *Journal of the Mechanics and Physics of Solids* 29 (1981) No. 2 pp. 115-142.
- [6] Häggblad, H.-Å. et al.: Formulation of a finite element model for localization and crack initiation in components of ultra-high strength steels, Hot sheet metal forming of high performance steel, June 15-17 2009. Luleå: Verlag Wissenschaftliche Scripten, 2009, pp. 229-237.
- [7] Mori, T., Tanaka, K.: Average stress in matrix and average elastic energy of materials with misfitting inclusions. In: *Acta Metall.* 21 pp. 571-574
- [8] Eshelby, J.D.: The determination of the elastic field of an ellipsoidal inclusion, and related problems. In: *Proc. Roy. Soc. London Ser. A* 241 (1957) pp. 376-396
- [9] Doghri, I., Ouaar, A.: Homogenization of two-phase elasto-plastic composite materials and structures Study of tangent operators, cyclic plasticity and numerical algorithms. In: *International Journal of Solids and Structures* (2003) No. 40 pp. 1681-1712
- [10] Perdahcioglu, E.S., Geijselaers, H.J.M.: Constitutive modeling of two phase materials using the mean field method for homogenization. In: *International Journal of Materials and Forming* (2010)
- [11] Mura, T.: *Micromechanics of Defects in Solids*, second ed. Martinus Nijhoff Publishers, Dordrecht, The Netherlands.
- [12] Qu, J., Cherkaoui, M.: *Fundamentals of Micromechanics of Solids*. John Wiley & Sons, Inc. (2006)
- [13] Hori, M., Nemat-Nasser, S.: Double-inclusion model and overall moduli of multi-phase composites. In: *Mechanics of Materials* (1992) p.189-206
- [14] Lielens, G.: Micro-macro modeling of structured materials. Ph.D. thesis, UCL/FSA, Louvain-la-Neuve, Belgium
- [15] Unosson M., Buzaud, E.: Scalar and Vectorized User Defined Material Routines in LS-DYNA. Methodology Report, FOA Defence Research Establishment (2000)
- [16] Ottosen N.S., Ristinmaa M.: *The mechanics of Constitutive Modeling*. Elsevier, Amsterdam (2005)
- [17] Kajberg, J.; Lindkvist, G.: Characterization of materials subjected to large strains by inverse modeling based on in-plane displacement fields. In: *International Journal of Solids and structures* 41 (2004) No. 13, pp. 3439-3459.
- [18] Marder, A.R.: Deformation Characteristics of Dual-Phase Steels. In: *Metallurgical Transactions A* (1982) vol.13A

Affiliation

- [1] Division of Solid Mechanics, Luleå University of Technology, 971 87 Luleå, stefan.golling@ltu.se